ChemPubSoc Europe

DOI: 10.1002/chem.201402515

CHEMISTRY A European Journal Full Paper

Transition-Metal Catalysis

An Operando FTIR Spectroscopic and Kinetic Study of Carbon Monoxide Pressure Influence on Rhodium-Catalyzed Olefin Hydroformylation

Christoph Kubis,[a] Mathias Sawall,[b] Axel Block,[a] Klaus Neymeyr,[a, b] Ralf Ludwig,[a, c] Armin Börner,[a, c] and Detlef Selent*[a]

Abstract: The influence of carbon monoxide concentration on the kinetics of the hydroformylation of 3,3-dimethyl-1-butene with a phosphite-modified rhodium catalyst has been studied for the pressure range $p(CO) = 0.20–3.83$ MPa. Highly resolved time-dependent concentration profiles of the organometallic intermediates were derived from IR spectroscopic data collected in situ for the entire olefin-conversion range. The dynamics of the catalyst and organic components are described by enzyme-type kinetics with competitive and uncompetitive inhibition reactions involving carbon monoxide taken into account. Saturation of the alkyl–rhodium intermediates with carbon monoxide as a cosubstrate occurs between 1.5 and 2 MPa of carbon monoxide pressure, which brings about a convergence of aldehyde regioselectivity. Hydrogenolysis of the acyl intermediate is fast at 30 °C and low pressure of $p(CO) = 0.2$ MPa, but is of minus first order with respect to the solution concentration of carbon monoxide. Resting 18-electron hydrido and acyl complexes that correspond to early and late rate-determining states, respectively, coexist as long as the conversion of the substrate is not complete.

Introduction

Olefin hydroformylation is a long-known catalytic process with industrial importance and sustained academic activities. Although the reaction was discovered with catalytically active species containing cobalt as the metal center, it acquired intensified academic interest when the higher activities of rhodium-based catalysts became evident.[1] A mechanistic rationale has been developed.[2] Recent work concentrates on widening the substrate scope and ligand development, but also on the utilization of nonclassical metals and renewable olefin feedstock and on the immediate transformation of aldehydes into secondary products, for example, by reduction.[3] However, the well-established class of phosphite-modified rhodium catalyst remains in the spotlight of research so far because, in part, of their potential for technical applications.[4] These catalysts show outstanding activities under mild reaction conditions and the capability to fulfill a plurality of requests regarding substrate tolerance and chemo- and aldehyde regioselectivities.[5] Still, a lot of interesting detail remains to be elucidated with respect to the kinetic and mechanistic specifics of hydroformylation catalysis. Spectroscopic investigations performed in situ are especially helpful for this purpose.[6] Thus, with the help of FTIR spectroscopy, it has recently become possible to detect an acyl complex that belongs to the class of diphosphite-modified rhodium catalysts under the conditions of the hydroformylation reaction.[7] For monophosphite rhodium catalysts, the coexistence of the electronically saturated hydrido–rhodium complex **1** and the acyl–rhodium complex **7** (Scheme 1) within a broad hydrogen pressure and olefin-conversion range has been proven and quantified.[8] Further results from our laboratory furnished evidence of an axial coordination of the phosphite ligand *trans* to the acyl group present in **7**,[8] a structural detail not anticipated in recent theoretical investigations.[9]

Complementary to the former work on rhodium catalysts modified with a bulky monophosphite ligand, we address herein, in more detail, the effects that occur from the influence of the carbon monoxide concentration on the reaction kinetics. A negative order has been reported for unmodified rhodium

[a] Dr. C. Kubis, A. Block, Prof. Dr. K. Neymeyr, Prof. R. Ludwig, Prof. Dr. A. Börner, Dr. D. Selent
Leibniz-Institut für Katalyse e.V.
Universität Rostock, Albert-Einstein-Str. 29a
18059 Rostock (Germany)
Fax: (+49) 381-128151169
E-mail: detlef.selent@catalysis.de

[b] Dr. M. Sawall, Prof. Dr. K. Neymeyr
Institut für Mathematik
Universität Rostock, Ulmenstr. 69
18057 Rostock (Germany)

[c] Prof. R. Ludwig, Prof. Dr. A. Börner
Institut für Chemie
Universität Rostock, Albert-Einstein-Str. 3
18059 Rostock (Germany)

Supporting information for this article is available on the WWW under http://dx.doi.org/10.1002/chem.201402515. It contains concentration profiles for the metal-containing complexes and organic components for all the carbon monoxide pressures applied as well as a detailed description of the handling of the Michaelis–Menten-type kinetics with competitive and uncompetitive equilibria, and the Christiansen formalism.

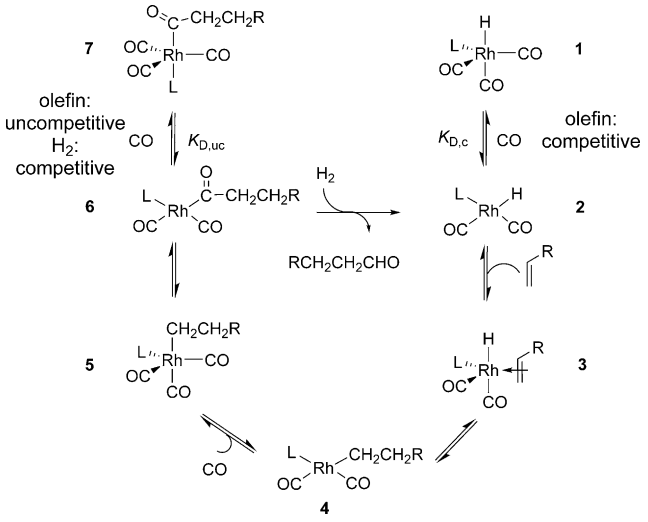

Scheme 1. Dissociative mechanism of the bulky monodentate phosphite ligand (L)-modified rhodium-catalyzed olefin hydroformylation. The pathway to the normal aldehyde, with only one ligand coordinated to the rhodium center, is depicted.

catalysis and monophosphite-modified systems, which were based on initial reaction rates determined at carbon monoxide pressures equal to or higher than 1 MPa.[10]

At lower pressures, positive reaction orders have been reported.[11] A plausible explanation is the depopulation of the saturated formally inactive complexes **1** and **7** to the benefit of reactive intermediates **2** and **6**, respectively. For **2**, the olefin competes with carbon monoxide, thus giving intermediates **3** and **4**. The formation of rhodium–alkyl compound **5** and also a subsequent carbonyl insertion toward unsaturated acyl complex **6** benefit from an enhanced concentration of carbon monoxide. Increasing the *p*(CO) affords a decrease of the population of **6** by shifting the equilibrium to species **7**. This inhibiting effect is uncompetitive with respect to the olefin but directly influences the rate of hydrogenolytic product formation.

We present herein new results for the tris(2,4-di-*tert*-butylphenyl)phosphite-modified rhodium catalyst applied to the hydroformylation reaction of 3,3-dimethyl-1-butene, an olefin considered to be a suitable model substrate for kinetic and mechanistic investigations. This work represents a continuation of a preceding report that dealt with a comprehensive spectroscopic characterization of respective rhodium complexes and kinetic analysis of the influence of the olefinic substrate and the cosubstrate dihydrogen.[8] Our current contribution focuses on the effect of carbon monoxide on the reaction kinetics, molar fractions of the catalytic species, and regioselectivity. Time-dependent concentration profiles are the experimental basis for this study. Such profiles were determined for the full olefin-conversion range for the organic components and the rhodium–hydride and acyl complexes that are present in submillimolar concentrations by FTIR spectroscopic analysis performed in situ. The changes of the individual concentrations with time are in accord with a model analogue of enzyme-type kinetics, in which catalyst saturation with carbon monoxide occurs and inhibition of olefin coordination and rhodium–acyl hydrogenolysis are both of relevance for the product-formation rate within a broad range of the carbon monoxide partial pressure.

Results and Discussion

Kinetic parameters, selectivity, and concentration profiles

The hydroformylation reaction was carried out at 30 °C in the range $p(CO) = 0.20–3.83$ MPa with a constant hydrogen pressure of 1.0 MPa applied. 3,3-Dimethyl-1-butene was chosen as a substrate that is incapable of double-bond isomerization, thus preventing undesired alteration of the kinetics.[12] Only 4,4-dimethylpentanal and 2,3,3-trimethylbutanal can be formed as hydroformylation products (Scheme 2). The rhodium concentration was set to 0.3 mM and the initial concentration of the substrate was 0.45 M. The low temperature is suitable for a detailed kinetic analysis because the catalyst system is extremely active at higher temperatures, thus leading to difficulties in controlling the reaction conditions. However, previous studies have shown that the basic kinetic features are similar for applied temperatures of 30 and 70 °C.[7]

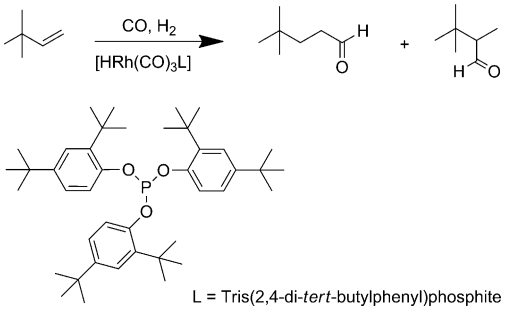

Scheme 2. Hydroformylation of 3,3-dimethyl-1-butene.

At the beginning of every batch, the catalyst precursor [Rh(acac)(CO)$_2$] (acac = acetylacetonate) was converted in the presence of 20 equivalents of monophosphite ligand into a mixture of the known hydrido complex *e*-[HRh(CO)$_3$(phosphite)] ($\tilde{\nu}$(CO) = 2015, 2043, 2093 cm^{-1}) and *e,e*-[HRh(CO)$_2$(phosphite)$_2$] ($\tilde{\nu}$(CO) = 2028, 2068 cm^{-1}) under the intended reaction conditions. The presence, identity, and basic geometric features of the latter hydride have been clearly evidenced recently by combining experimental FTIR spectroscopic data and DFT calculations.[8] After a complete precursor-to-catalyst transformation, the olefin was added, which was taken as the reaction start.

The full sequence of each batch, including the transformation of the precursor into the rhodium–hydride complexes, the olefin addition, and the following reaction progress, was followed by FTIR spectroscopic analysis. The experimental setup consisted of a stainless-steel autoclave with a constant pressure controller. The autoclave was connected with a high-pressure transmission IR cell and an automatic sampling device to take liquid samples for GC analysis. Because of the very low

catalyst concentration applied, a wedged spacer was placed between the ZnS windows of the transmission IR cell to prevent the disturbing interference fringes that otherwise occurred in the IR spectra.[13] Further experimental details are given in the Experimental Section.

The hydroformylation reactions performed showed high chemoselectivities toward the aldehydes; only trace amounts (< 0.5%) of alcohols were found. For the batch performed at 1 MPa CO/1 MPa H_2, the aldehyde products were formed with constant regioselectivity, as verified by online sampling and GC analysis (see the Supporting Information). By assuming the same kinetics for both products with any other p(CO) value applied, we used the sum of the normal and iso aldehyde concentrations for the following kinetic analysis of all the batches.

The effect of the variation of the carbon monoxide pressure on the product formation is shown in Figure 1. At a pressure of 0.2 MPa of CO, a turnover frequency of 1065 h^{-1}, based on

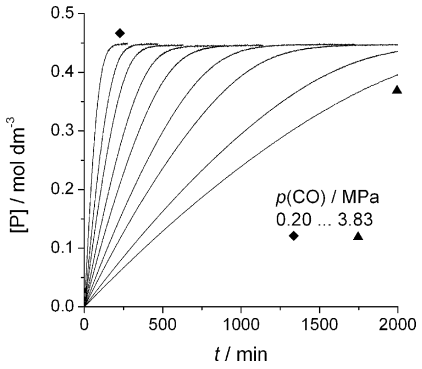

Figure 1. Influence of carbon monoxide pressure on aldehyde product formation (P = normal + iso isomers) in the hydroformylation of 3,3-dimethyl-1-butene in *n*-hexane with a Rh/tris(2,4-di-*tert*-butylphenyl)phosphite catalyst (p(CO) = 0.20, 0.35, 0.50, 0.75, 0.99, 1.49, 1.99, 2.98, 3.83 MPa (plots follow the same sequence); [Rh] = 0.3 mM; $[olefin]_0$ = 0.45 M). Experimental data from FTIR spectroscopic analysis were acquired after mixing for 270 s. Time intervals between the IR spectroscopic measurements were 37 s for the first 120 min of each batch and 67 s after that period. See the Supporting Information for a comparison of the data obtained by IR spectroscopic analysis with that from GC analysis.

the initial rate, was determined. This result means that the reaction is still fast despite the uncommonly low temperature applied. By progressively increasing the carbon monoxide pressure, the reaction decelerates; consequently, for the batches run at 2.98 and 3.83 MPa, full conversion was not achieved even after more than 30 hours of reaction time.

A fit of the numerically integrated Michaelis–Menten equation [Eq. (1)] was performed to all of the product concentration profiles from Figure 1. Table 1 summarizes the kinetic values obtained from this fit together with data for the product selectivity. The procedure of using the Michaelis–Menten equation for determining the saturation rate V_{sat}^{obs} and the Michaelis constant K_m^{obs} from the product-concentration profiles that cover the entire conversion range has been validated.[8] The regression results of this work are given in the Supporting Information. The initial rates can be calculated from the kinetic parameters and the respective initial concentration of the olefinic substrate [Eq. (2)].

Table 1. Kinetic values for the hydroformylation of 3,3-dimethyl-1-butene with the Rh/tris(2,4-di-*tert*-butylphenyl)phosphite catalyst at 30 °C ($p(H_2)$ = 1 MPa).

p(CO) [mPa]	[CO][a] [mol dm^{-3}]	V_{sat}^{obs} [mol dm^{-3} min^{-1}]	k'_{obs}[b] [min^{-1}]	K_m^{obs} [mol dm^{-3}]	Selectivity[c] [*n*/iso]
0.20	0.022	7.59×10^{-3}	25.5	0.196	0.95:0.05
0.35	0.039	3.89×10^{-3}	13.1	0.155	0.93:0.07
0.50	0.057	2.96×10^{-3}	9.2	0.143	0.92:0.08
0.75	0.084	1.79×10^{-3}	5.9	0.137	0.91:0.09
1.00	0.113	1.39×10^{-3}	4.6	0.139	0.90:0.10
0.99	0.112	1.31×10^{-3}	4.5	0.138	0.90:0.10
1.49	0.169	0.89×10^{-3}	3.0	0.130	0.89:0.11
1.99	0.228	0.67×10^{-3}	2.3	0.132	0.88:0.12
2.98	0.347	0.44×10^{-3}	1.5	0.129	0.88:0.12
3.83	0.451	0.34×10^{-3}	1.2	0.130	0.88:0.12

[a] Solution concentrations of CO refer to the amount of pure solvent used for the experiments and have been calculated from data given in: R. Koelliker, H. Thies, *J. Chem. Eng. Data* **1993**, *38*, 437–440. [b] Ratio of V_{sat}^{obs}/[Rh]. [c] Derived from GC data.

$$V = \frac{d[P]}{dt} = \frac{V_{sat}^{obs}[S]}{K_m^{obs} + [S]} = \frac{V_{sat}^{obs}([S]_0 - [P])}{K_m^{obs} + ([S]_0 - [P])} \quad (1)$$

$$V_0 = \frac{V_{sat}^{obs}[S]_0}{K_m^{obs} + [S]_0} \quad (2)$$

Initially, the increase of p(CO) affords higher amounts of the iso product. Such an effect is known[10a,14] and has been discussed to originate from a reduced tendency to undergo β-hydride elimination and a favored carbon monoxide addition/insertion reaction of the isoalkyl analogue of intermediate **4** (Scheme 1), provided that the normal and iso acyl complexes undergo subsequent hydrogenolysis at the same rate.[15] But, our results also verify a constancy of selectivity if p(CO) = 1.5 MPa or higher, a result that is not deduced easily from the accepted mechanism. The change of selectivity depicted in Figure 2 roughly parallels the known equilibrium shift between saturated hydrides **1** and $[HRh(CO)_2(phosphite)_2]$,[8,16] thus suggesting that the latter represents the more selective catalyst. However, there is no evidence that this bisphosphite complex contributes to product formation at all. Also, the relevant acyl complex remains unknown. With a quick equilibrium that occurs between both hydrides taken into account, **1** may mainly act as the catalyst. Then, the convergence of selectivity probably is due to catalyst saturation with carbon monoxide as a cosubstrate. The respective results and discussion are given in Figure 9.

The evolution in the metal carbonyl region of the FTIR spectra with ongoing reaction time is shown for two batches performed at the extremes of the carbon monoxide pressure applied (i.e., 0.20 and 3.83 MPa; Figure 3). The acyl complex $[C_6H_{13}C(O)Rh(CO)_3(phosphite)]$ dominates directly after olefin addition for both batches. This complex most probably is a mixture of normal and iso regioisomers that could not be resolved

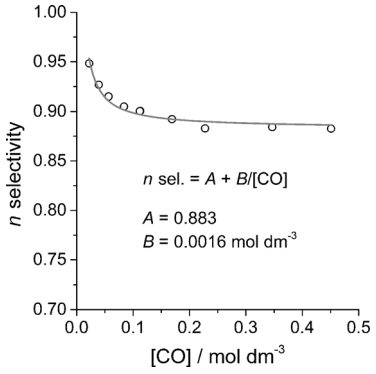

Figure 2. Influence of carbon monoxide concentration on the normal(*n*) selectivity for the hydroformylation of 3,3-dimethyl-1-butene in *n*-hexane with a Rh/tris(2,4-di-*tert*-butylphenyl)phosphite catalyst at 30 °C and 1 MPa H_2 ([Rh] = 0.3 mM; [ligand]/[Rh] = 20:1; $[olefin]_0$ = 0.45 M). The experimental data were obtained from GC analysis.

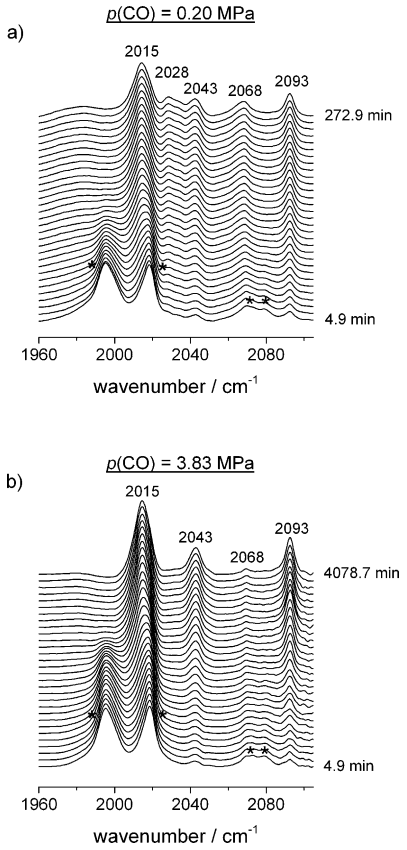

Figure 3. FTIR spectra for selected carbon monoxide pressures in the IR metal carbonyl region during the hydroformylation of 3,3-dimethyl-1-butene in *n*-hexane with a Rh/tris(2,4-di-*tert*-butylphenyl)phosphite catalyst ([Rh] = 0.3 mM; [ligand]/[Rh] = 20:1; $[olefin]_0$ = 0.45 M). Asterisks indicate the acyl complex formed after the addition of the olefin at t = 0 min ($\tilde{\nu}$(CO) = 1995, 2019, 2072 and 2079 cm^{-1}). $[HRh(CO)_3(phosphite)]$ (main component): $\tilde{\nu}$(CO) = 2015, 2043, 2093 cm^{-1}; $[HRh(CO)_2(phosphite)_2]$ (minor component): $\tilde{\nu}$(CO) = 2028, 2068 cm^{-1}. Please note the different reaction times.

by IR spectroscopic analysis in the shown spectral range. The complex depletes much more quickly at 0.20 MPa, thus leading to a mixture of the above-mentioned hydrido complexes (Figure 3a). For better insight into the superposition and dynamics of the experimental spectra, chemometrical treatment based on factor analysis was performed. In analogy to our former work, the pure component decomposition (PCD) algorithm was applied.[17,8] Interestingly, the individual spectra of **1** and the related bisphosphite complex could not be resolved. This result indicates that an equilibrium between both hydrides occurs, which is fast with respect to hydroformylation kinetics. As a consequence for the kinetic analysis, it is appropriate to apply the quasiequilibrium approximation with the hydrido complexes treated as a pseudocomponent. However, it has been possible to determine the ratio of **1**/$[HRh(CO)_2(phosphite)_2]$, which depends on the partial pressure of carbon monoxide. In the absence of the olefin, we estimated values of 2.3 and 32.3 for p(CO) = 0.20 and 3.83 MPa at an molar ratio P/Rh = 20:1 from reported data.[8] In contrast, the IR spectrum of the acyl complex shows no dependency on carbon monoxide pressure (Figure 4a, b). For all the carbon monoxide pressures, the spectrum fits to that assigned to a structure with the phosphite moiety coordinated in an axial position *trans* to the acyl moiety, with three carbon monoxide ligands occupying equatorial positions in the trigonal-bipyramidal complex geometry.[8] Therefore, this structure turns out to be significantly more stable than any substitution product

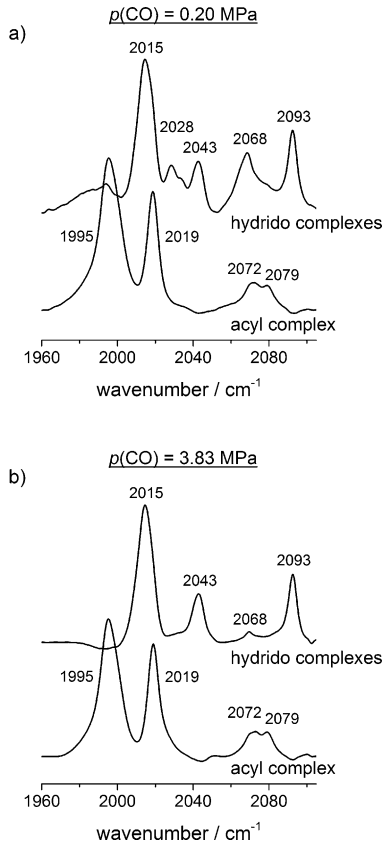

Figure 4. FTIR spectra of mixtures of $[HRh(CO)_3(phosphite)]$ and $[HRh(CO)_2(phosphite)_2]$ (hydrido complexes) and $[C_6H_{13}C(O)Rh(CO)_3(phosphite)]$ (acyl complex). The spectra were obtained from catalytic batches with p(CO) = 0.20 and 3.83 MPa (see Figure 3 for further experimental conditions).

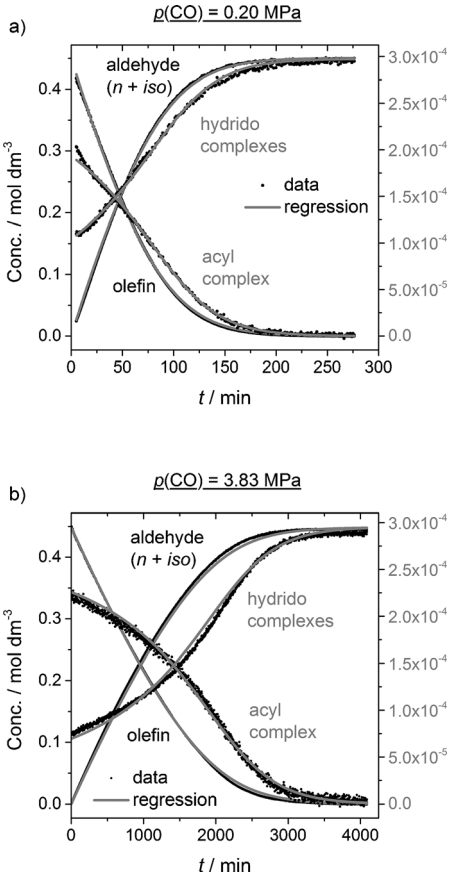

Figure 5. Experimental concentration profiles of the olefin and aldehydes for a) $p(CO) = 0.2$ and b) 3.83 MPa, as obtained conventionally by FTIR spectroscopic analysis and profiles of the organometallic components from PCD. (----) Least-squares fit by using the Michaelis–Menten kinetic model.[20] The concentration range of the rhodium complexes is given by the right-hand axis. Hydroformylation of 3,3-dimethyl-1-butene in *n*-hexane with a Rh/tris(2,4-di-*tert*-butylphenyl)phosphite catalyst ([Rh] = 0.3 mM; [ligand]/[Rh] = 20:1; $[olefin]_0 = 0.45$ M; $p(H_2) = 1.0$ MPa).

in which the phosphorus ligand has entered the equatorial plane.[18]

The consequence of the variation of [CO] on the reaction kinetics is illustrated by the concentration profiles that include pure organic components and also the observable rhodium complexes. Such profile sets were determined for the entire olefin-conversion range for all the experiments. Figure 5 shows two selected sets of profiles obtained at $p(CO) = 0.2$ and 3.83 MPa, respectively. Each individual profile is accompanied by the result of a simultaneous integration/regression of the set of ordinary differential Equations (3a–d) derived from the Michaelis–Menten mechanism depicted in Scheme 3, where (Cat) and (CatS) represent pseudocomponents, which consist of the 16- and 18-electron hydrido and acyl–rhodium complexes, respectively, at quasiequilibrium. Seven additional sets of concentration profiles for the other carbon monoxide partial pressures applied are given in the Supporting Information.

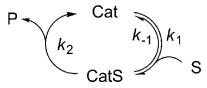

Scheme 3. Michaelis–Menten mechanism. Cat = catalyst: hydrido–rhodium complexes; CatS = catalyst–substrate complex: acyl–rhodium complexes; S = olefinic substrate; P = product aldehyde. The pseudocomponent approach, which also includes bisphosphite hydrido complexes, applies.

$$\frac{d[S]}{dt} = -k_1[S][Cat] + k_{-1}[CatS] \quad (3a)$$

$$\frac{d[Cat]}{dt} = -k_1[S][Cat] + k_{-1}[CatS] + k_2[CatS] \quad (3b)$$

$$\frac{d[CatS]}{dt} = k_1[S][Cat] - k_{-1}[CatS] - k_2[CatS] \quad (3c)$$

$$\frac{d[P]}{dt} = k_2[CatS] \quad (3d)$$

It can be seen from Figure 5 that all the experimental data are reconstructed conveniently by the kinetic model, which holds not only for the concentration profile of 3,3-dimethyl-1-butene and the aldehyde products, but also for the observable rhodium complexes. Notably, it was verified once more that the hydrides and acyl complex $[C_6H_{13}C(O)Rh(CO)_3(phosphite)]$ (**7**) coexist over the full conversion range. At the reaction start, with a high olefin concentration given, the latter dominates. With an ongoing reaction, the fraction of the hydrides increases. Interestingly, the initial molar fraction of **7** is only slightly influenced by the carbon monoxide pressure, thus rising from 0.7 to 0.77 at $p(CO) = 0.2$ and 3.83 MPa, respectively (Figure 6a). This outcome is in accord with the uncompetitive and competitive inhibition reactions that occur in this catalytic cycle (see below). From the data given in Figure 5, further quantitative information can be derived. The concentration of the rhodium–acyl complex, shown for nine different CO partial pressures in Figure 6a, is linearly correlated with the rate of aldehyde formation (Figure 6b). A negative order with respect to $p(CO)$ for acyl hydrogenolysis is thus proven.[19] These relationships hold for the full carbon monoxide pressure range applied, even below 1 MPa, and for the full concentration range for which the acyl complex is observable.

The experimental results presented above are in accord with the established interpretation of the hydroformylation mechanism. Changes of the equilibrium between **6** and **7** are likely to occur upon pressure variation, thus enhancing the fraction of the undetected, but catalytically essential intermediate **6** at low carbon monoxide pressures.

We want to emphasize that the analysis of the reaction rates with the help of the acyl complex, as performed here, is a challenge and not very common in homogeneous transition-metal catalysis. The determination of a direct correlation of rate with the mass balance of catalytic intermediates can be hampered due to chemical reasons, for example, a very low concentration of the catalyst–substrate complex and also by various methodological aspects.

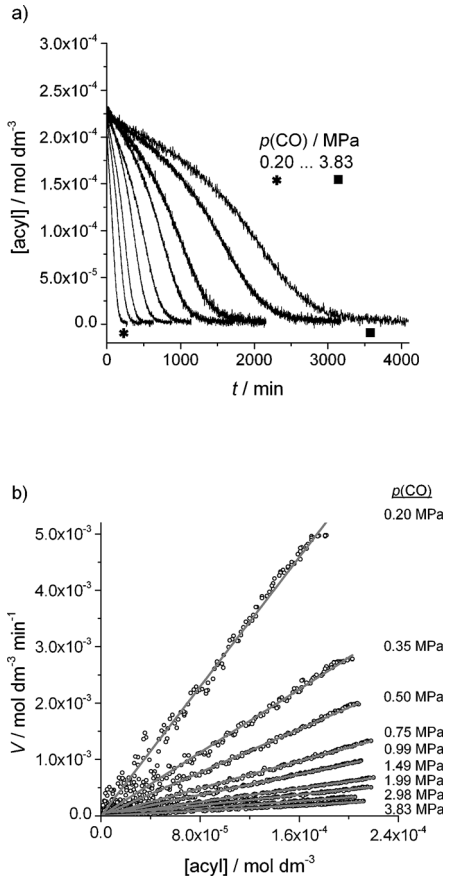

Figure 6. Dependency from carbon monoxide pressure. a) Concentration profiles of the rhodium–acyl complex. b) Plots of the rate of product formation versus the concentration of the acyl complex. Hydroformylation of 3,3-dimethyl-1-butene in *n*-hexane with a Rh/tris(2,4-di-*tert*-butylphenyl)phosphite catalyst ([Rh] = 0.3 mM: [olefin]$_0$ = 0.45 M; [ligand]/[Rh] = 20:1).

Uncompetitive and competitive inhibition, the Michaelis constant, and catalyst saturation with CO

Our treatment of the hydroformylation reaction, with special emphasis on the dependency of the rate of product formation from the carbon monoxide concentration, follows the Christiansen formalism.[21] The competitive and uncompetitive equilibria assigned in Scheme 1, which involve the cosubstrate carbon monoxide, complexes **2** and **1**, and complexes **6** and **7**, respectively, have been incorporated. The general expression obtained is represented by Equation (4), where k_{obs} is the pseudoconstant of irreversible acyl complex hydrogenolysis. The constants $K_{D,c}$ and $K_{D,uc}$ represent the dissociation constants of competitive and uncompetitive inhibition. The J value results from the fact that carbon monoxide acts as a cosubstrate and is composed of distinct rate constants and the concentration of the substrate hydrogen (see the Supporting Information for more details). Equation (5) is derived from Equation (4), it represents the Michaelis–Menten equation with composed kinetic parameters, and was used to determine the values of V_{sat}^{obs} and K_m^{obs} depicted in Table 1.

$$V = \frac{k_{obs}[Cat]_0[S]}{\left(1+\frac{[CO]}{K_{D,c}}\right)\left(K_m+\frac{J}{[CO]}\right)+\left(1+\frac{[CO]}{K_{D,uc}}\right)[S]} \quad (4)$$

$$V = \frac{\left\{k_{obs}[Cat]_0/\left(1+\frac{[CO]}{K_{D,uc}}\right)\right\}[S]}{\left\{\left(1+\frac{[CO]}{K_{D,c}}\right)\left(K_m+\frac{J}{[CO]}\right)/\left(1+\frac{[CO]}{K_{D,uc}}\right)\right\}+[S]} = \frac{V_{sat}^{obs}[S]}{K_m^{obs}+[S]} \quad (5)$$

Equations (6) and (7) result when $[S] \gg K_m^{obs}$. With the help of the experimental values of k'_{obs}, an estimate of k_{obs} and $K_{D,uc}$ or of $1/K_{D,uc} = K_{Inh,uc}$, respectively, should be possible by plotting $1/k'_{obs}$ versus [CO] (such a plot is given in Figure 7a). A line through the origin was obtained, thus indicating a hydrogenolysis of minus first order with respect to the carbon monoxide concentration within the whole pressure range applied. A linear regression of $\ln(k'_{obs})$ versus $\ln([CO])$ gives an order of reaction with respect to the carbon monoxide concentration of −1.02. The fact that a line through the origin was found identifies a very large value for $K_{Inh,uc}$ and that the inequation 1/

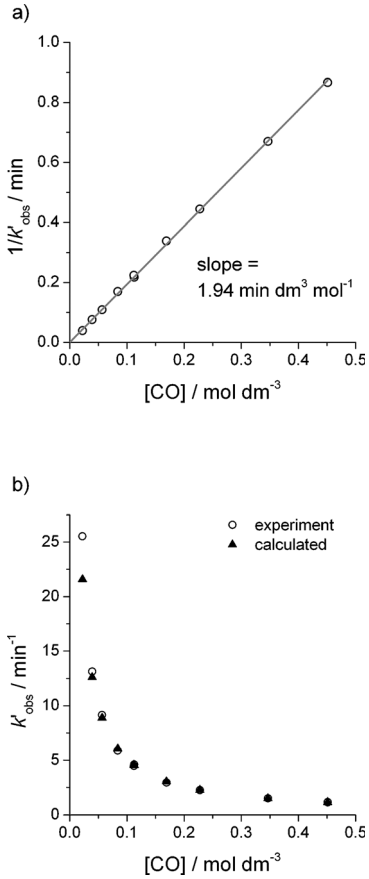

Figure 7. a) Linear regression: reciprocal observed rate constants k'_{obs} versus carbon monoxide concentration. b) Comparison of experimental values of k'_{obs} (open circles) with that obtained by using the ratio $K_{Inh,uc}/k_{obs}$. Hydroformylation of 3,3-dimethyl-1-butene in *n*-hexane with a Rh/tris(2,4-di-*tert*-butylphenyl) phosphite catalyst ([Rh] = 0.3 mM; [olefin]$_0$ = 0.45 M; [ligand]/[Rh] = 20:1).

$K_{D,uc} \times [CO] = K_{Inh,uc} \times [CO] \gg 1$ is valid already at very low CO pressures. This result can be considered to be the reason for the spectroscopic observation of the coordinatively saturated 18-electron acyl complex only, with the consequence that the corresponding unsaturated complex is present only in undetectable concentrations. As a result, no distinct numerical values can be determined for k_{obs} and $K_{Inh,uc}$, but the ratio $K_{Inh,uc}/k_{obs}$ is accessible. This ratio is part of Equation (8), which allows for the calculation of the composed rate constant k'_{obs}. The comparison between the calculated and experimental values of this constant (depicted in Figure 7b) shows a good agreement.

$$\frac{V_{sat}^{obs}}{[Cat]_0} = \frac{k_{obs}}{\left(1 + \frac{[CO]}{K_{D,uc}}\right)} = k'_{obs} \tag{6}$$

$$\frac{1}{k'_{obs}} = \frac{1}{k_{obs}} + \frac{1}{k_{obs} K_{D,uc}} [CO] \tag{7}$$

$$\frac{1}{k'_{obs}} = \frac{K_{Inh,uc}}{k_{obs}} [CO] \tag{8}$$

It would be interesting to see if additional information on the influence of carbon monoxide partial pressure arises when the analysis is based on the initial reaction rate. Our finding with respect to the uncompetitive inhibition with carbon monoxide as an inhibitor was based on the V_{sat}^{obs} value of the saturation rate. This rate is the highest possible product-formation rate in which all of the catalyst is complexed with the olefin (S = reference substrate); namely, $[CatS] = [Cat]_0$. This rate can only be approached if the relation $[S] \gg K_m^{obs}$ is valid. The initial rate represents the reaction rate at the initial olefin concentration $[S]_0$ applied [Eq. (2)]. The initial rate can be close to that at catalyst saturation or smaller, and it directly corresponds to the relation between the $[S]_0$ and K_m^{obs} values; because carbon monoxide acts as a substrate as well, this circumstance should result in a positive influence on the product-formation rate.

To check this hypothesis, initial rates were calculated by using Equation (2) with the values V_{sat}^{obs} and K_m^{obs} determined for selected initial substrate concentrations. The slope of a double logarithmic plot of $\ln(V_0)$ versus $\ln([CO])$ gave the value for the order of reaction with respect to [CO] for each experiment. A plot of these reaction orders versus olefin concentration is shown in Figure 8.

As a first result obtained for $[S]_0 = 0.45$ M, no significant difference is seen relative to the result derived from the saturation rate at the initial olefin concentration, which was applied for the experimental batches. A reaction order of -0.99 with respect to [CO] was calculated, but the order of reaction increases and partial orders in [CO] result with decreasing substrate concentration. Such partial orders based on initial rates have been reported for other hydroformylation catalysts.[11] At least for the reaction system under study here, we deduced a shift in the relation between the $[S]_0$ and K_m^{obs} values. The reason for this shift is detailed below.

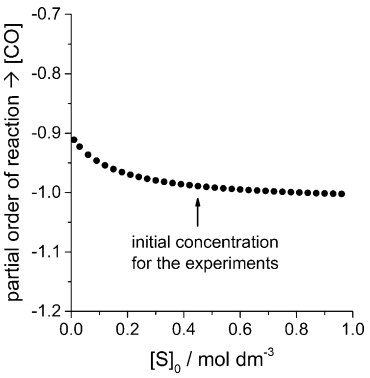

Figure 8. Partial order of reaction with respect to the concentration of carbon monoxide for selected substrate concentrations. The calculation is based on the experimentally determined parameters V_{sat}^{obs} and K_m^{obs} and Equation (2).

The origin for the dependency depicted in Figure 8 is found in the influence of [CO] on the Michaelis constant K_m^{obs}. This constant is defined by Equation (9), which represents a part of Equation (5). It consists of factors α, α', and the term β, which account for the competitive and uncompetitive inhibition by carbon monoxide and the role of carbon monoxide as a cosubstrate itself. Equation (10) results from $1/K_{D,uc} \times [CO] \gg 1$ and $1/K_{D,c} \times [CO] \gg 1$. Thus, this equation respects the fact that only the saturated hydrido and acyl complexes, respectively, can be detected spectroscopically. Both the uncompetitive and competitive inhibition equilibria are shifted largely to the side of the 18-electron complexes.

$$K_m^{obs} = \frac{\left(1 + \frac{[CO]}{K_{D,c}}\right)\left(K_m + \frac{J}{[CO]}\right)}{\left(1 + \frac{[CO]}{K_{D,uc}}\right)} = \frac{\alpha(K_m + \beta)}{\alpha'} \tag{9}$$

$$K_m^{obs} = K_m \frac{K_{D,uc}}{K_{D,c}} + \frac{K_{D,uc}}{K_{D,c}} J \frac{1}{[CO]} = A + B\frac{1}{[CO]} \tag{10}$$

The dependency of the K_m^{obs} values on the carbon monoxide concentration is characterized by the constants A and B, which were derived from a regression of the plot of the experimental values of the observed Michaelis constant given in Table 1 versus the carbon monoxide concentration (Figure 9). It can be seen that the K_m^{obs} value first decreases and then approaches a plateau with $[CO] \gg B$. This dependency shows very nicely that the K_m^{obs} constants deliver information on the role of carbon monoxide as a cosubstrate by having a slightly positive effect on the product-formation rate. Considering the Michaelis–Menten equation [Eq. (1)], the Michaelis constant is a term in the denominator, so a decrease of the K_m^{obs} constants leads to an increase of the reaction rate. However, this positive effect is small because any increase in carbon monoxide concentration enforces uncompetitive inhibition and promptly reduces the rate of acyl hydrogenolysis.

Mechanistically, the influence of [CO] on the K_m^{obs} constant can be understood in terms of a Michaelis–Menten-type cata-

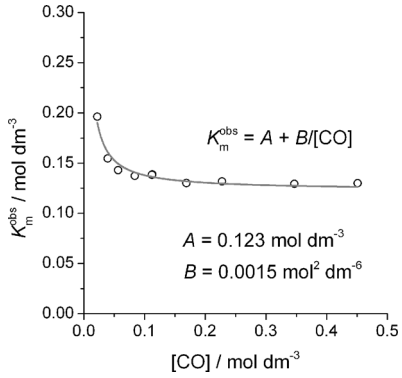

Figure 9. Plot of the observed Michaelis constant versus carbon monoxide concentration and regression according to Equation (10). Hydroformylation of 3,3-dimethyl-1-butene in *n*-hexane with a Rh/tris(2,4-di-*tert*-butylphenyl)-phosphite catalyst ([Rh] = 0.3 mM; $[olefin]_0$ = 0.45 M; [ligand]/[Rh] = 20:1).

lyst saturation with the cosubstrate carbon monoxide. The relevant part in the reaction mechanism is the coordination of carbon monoxide to the unsaturated 16-electron alkyl complex **4**, thus yielding the respective saturated 18-electron complex **5**, which subsequently undergoes CO insertion to give the 16-electron acyl complex **6**. This consideration is represented by Equation (11), which arises from Equation (10), and is structurally identical to the Michaelis–Menten equation. The saturation regime related to carbon monoxide is reached already at [CO] = 0.2 M, thus representing a ratio of [CO]/[Rh] = 667:1 for our experiments. No significant change of the K_m^{obs} constant is observed with a further increase of the CO pressure (or CO/Rh ratio).

$$\frac{1}{K_m^{obs}} = \frac{[CO]}{B + A[CO]} = \frac{(1/A)[CO]}{(B/A) + [CO]} \tag{11}$$

With the analysis of the Michaelis constant given herein, the small positive influence of carbon monoxide on the product-formation rate is disclosed elegantly. To the best of our knowledge, a similar study has not been reported.

By comparing Figures 2 and 9, one can see a similar trend for the effect of [CO] not only on the Michaelis constant but also on the *n*-selectivity. Both dependencies are described by an equation of the type $y = A + B/[CO]$, which may indicate that regioselectivity is also influenced by a saturation process that occurs with carbon monoxide. Such a suggestion is plausible, that is, that with a large excess of carbon monoxide present, the unsaturated normal and iso alkyl complexes **4** become saturated with carbon monoxide and β-hydride elimination is suppressed. But, probably the respective equilibria remain highly mobile and fast with respect to product formation. Consequently, a plateau is reached for regioselectivity at high concentrations of carbon monoxide ($[CO] \gg B$). Thus, the changes of selectivity observed will not originate from an equilibrium shift between the 18-electron tricarbonyl complex **1** and $[HRh(CO)_2(phosphite)_2]$, which occurs upon pressure variations and can easily be followed by IR spectroscopic analysis, but rather from variations of the concentration of the up-to-now undetected 16-electron alkyl intermediates. Whereas at the higher temperatures applied (i.e., 100 °C), the formation of linear and branched rhodium–alkyl complexes was still reversible at 2 MPa of carbon monoxide applied, and the regioselectivity was mainly determined by the entropy change that occurs during the formation of the rhodium–alkyl complex for the same reaction system,[4d] saturation phenomena that occur with carbon monoxide will strongly interfere when the reactions are performed at ambient temperature.

The fact that the experimentally determined Michaelis constants can be described by Equation (10) can be regarded as indirect proof for the existence of competitive inhibition. In the case that inhibition does not play any role, this equation will have another form because of the α factor is then absent in the foregoing Equation (9). The Michaelis constant should further decrease with higher carbon monoxide concentrations; such a dependency was not observed. The occurrence of competitive inhibition is also in accord with the influence of [CO] on the initial molar fractions of the acyl complex and the hydrido complex already mentioned. These molar fractions were not changed for carbon monoxide concentrations greater than 0.2 M.[22] The reason for this outcome lies in the relationship between the K_m^{obs} constant at a given initial substrate concentration and the molar fractions of the catalyst and catalyst–substrate complex [Eq. (12)] and the dependency of the Michaelis constant on [CO] as depicted in Figure 9.

$$\frac{[S]_0}{K_m^{obs} + [S]_0} = \frac{[CatS]}{[CatS] + [Cat]} \tag{12}$$

We tried to get quantitative information with regard to the competitive inhibition reaction. Dividing K_m^{obs} by V_{sat}^{obs} eliminates the α' factor, which accounts for the uncompetitive inhibition in Equation (9). Equation (13) is obtained based on the assumption that $K_{Inh,c} \times [CO] \gg 1$.[23]

$$\frac{K_m^{obs}}{k'_{obs}} = \frac{K_m K_{Inh,c}}{k_{obs}}[CO] + \frac{K_{Inh,c} J}{k_{obs}} \tag{13}$$

The respective plot of K_m^{obs}/k'_{obs} versus [CO] is given in Figure 10. The linear dependency observed is in agreement

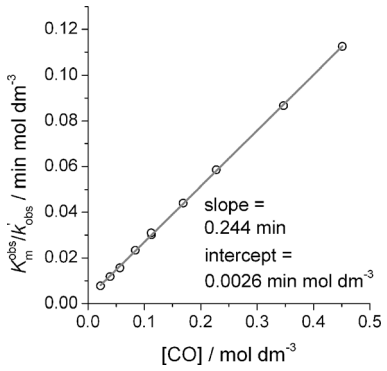

Figure 10. Plot of K_m^{obs}/k'_{obs} versus [CO]. Hydroformylation of 3,3-dimethyl-1-butene in *n*-hexane with a Rh/tris(2,4-di-*tert*-butylphenyl)phosphite catalyst ([Rh] = 0.3 mM; $[olefin]_0$ = 0.45 M; [ligand]/[Rh] = 20:1).

with the occurrence of competitive inhibition. However, no distinct values can be derived from the data for $K_{Inh,c}$, thus indicating a high preference for the electronically saturated hydrido complexes. The result found herein is analogous to that found for the inhibition involving the acyl complexes. Obviously, it is not possible at the moment to describe the uncompetitive and competitive equilibria comprehensively. The detection and quantification of the respective coordinatively unsaturated complexes involved will be required.

Conclusion

Precise time-resolved insight into the dynamics of the hydroformylation reaction of 3,3-dimethyl-1-butene has been provided by coupling GC, FTIR spectroscopic analysis performed in situ, and advanced chemometric treatment of IR spectra. Thus, detailed concentration profiles became accessible not only for the organic components, but also for the relevant rhodium complexes. These profiles have allowed a qualitative interpretation and a conclusive quantitative description of the relations between the concentrations of the rhodium complexes and the rate of product formation and on the dependency of these relations on the concentration of carbon monoxide.

Hydride and acyl complexes that correspond to early and late rate-determining states, respectively,[24] coexist for nearly the entire conversion range. The rate control shifts with conversion for the whole carbon monoxide pressure range applied. The two different hydrido–rhodium complexes observed by employing IR spectroscopy in situ cannot be distinguished kinetically, thus pointing to very fast equilibria for ligand exchange between these species. The acyl–rhodium complex, which can be regarded to be equipollent to the catalyst–substrate complex, with the olefin representing the reference substrate, could also be tracked quantitatively in a time-resolved manner. The rate of product formation from this compound shows a minus first-order dependency with respect to the carbon monoxide concentration.

The overall dynamics can be interpreted in terms of Michaelis–Menten kinetics involving competitive and uncompetitive side reactions, in which saturation of the catalyst occurs also with the cosubstrate carbon monoxide. An inhibiting influence of carbon monoxide on the reaction rate is found already at headspace partial pressures below 1 MPa.

In completion to earlier work, it can now be concluded that for all the substrates, that is, 3,3-dimethyl-1-butene, dihydrogen, and carbon monoxide, the same kinetic approach is applicable to describe their influence on the monophosphite-containing catalytic system, which is a rhodium-catalyst representative for the most active catalyts known for olefin hydroformylation. Similar concepts of enzyme-type kinetics have already earlier been found to be useful for homogeneous catalysis.[25] However, a comprehensive result, as provided herein, is not thus widespread, especially for the case in which the kinetic evaluation benefits from the direct observation of the catalyst–substrate complex.[26]

Experimental Section

Materials

3,3-Dimethyl-1-butene (>99%, GC) was purchased from Sigma–Aldrich (95%) and distilled in an argon atmosphere over sodium. The solvent *n*-hexane from Sigma–Aldrich (>99%) was distilled in an argon atmosphere over Sicapent (Merck). The internal GC standard dodecane (>99%, Sigma–Aldrich) was stored over Sicapent for drying and distilled under vacuum. The catalyst precursor [(acac)Rh(CO)$_2$] (39.46% Rh) from Umicore was used without further purification. The monophosphite ligand tris(2,4-di-*tert*-butylphenyl)phosphite (TDTBPP; 98%, Sigma–Aldrich) was used as obtained. The following gases were used: synthesis gas (CO/H_2 = 1:1, from 99.997% CO and 99.999% H_2, Linde), carbon monoxide (99.997%, Linde), hydrogen (99.9993%, Linde), and argon (99.999%, Linde). Bis(2,2,6,6-tetramethyl-4-piperidyl)sebaceate (Tinuvin 770 DF; 100%, Ciba) was used as a phosphite stabilizer and added in equimolar amounts with respect to the phosphite ligand.

Devices and procedures

For the HP FTIR spectroscopic measurements, the experimental setup consisted of a stainless-steel autoclave (200 mL) with a gas-entrainment impeller and an oil-bath thermostat (premex reactor AG; Leimen, Germany) equipped with a heatable transmission flow-through IR cell (Dr. Bastian Feinwerktechnik GmbH; Wuppertal, Germany) and an automatic sampling device (amplius GmbH; Rostock, Germany) to collect samples during the reaction for GC analysis (Figure 11).

For the circulation of the reaction solution between the reactor and the IR cell, a microgear pump (mzr-7255, HNP Mikrosysteme GmbH; Parchim, Germany) was used. Olefin injections were performed with the help of a six-port valve and a respective loop (Knauer GmbH; Berlin, Germany). FTIR spectra were collected on a Bruker Tensor 27 FTIR spectrometer with a MCT-A detector. The MCT detector was featured with a dewar, with a hold time of 24 h with liquid nitrogen as a cooling agent. Variations in band intensities that arise from a nonconstant detector signal due to N_2-level alteration and the refilling required for longer reaction times were

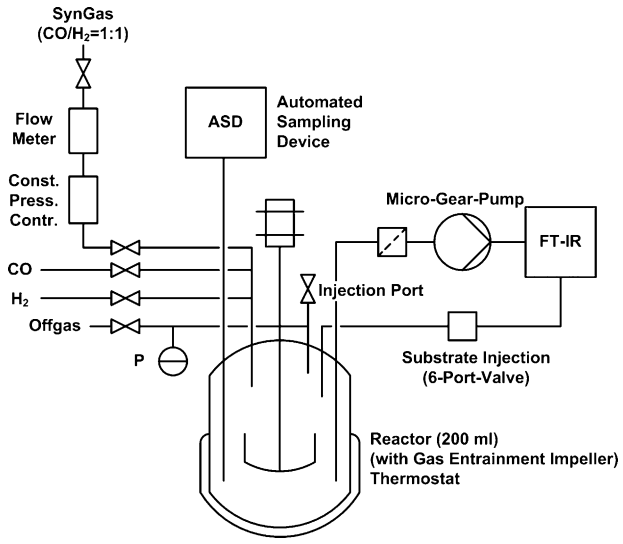

Figure 11. Experimental setup for catalytic batches, high-pressure FTIR spectroscopic measurements collected in situ, and automated sampling for GC analyses.

eliminated by the baseline-correction procedure. As a window material, ZnS (Korth Kristalle GmbH; Kiel, Germany) was used. The mean optical-path length was 0.48 mm, which resulted from a wedged spacer. The apparatus provided synthesis gas ($CO/H_2 = 1:1$), carbon monoxide, and hydrogen for pressurization. A constant-pressure controller (Brooks Instrument; Hatfield, PA, USA) was used for regulation of the consumed gas ($CO/H_2 = 1:1$).

Stock solutions were prepared from the solids by using Schlenk techniques. All the liquid components, except the olefin were transferred into the reactor. The stirrer speed was set to 1500 rpm and the speed of the microgear pump was set to 2333 rpm (displacement volume = 48 μL). At the reaction temperature of 30 °C, the system was pressurized with the respective partial pressure of carbon monoxide and 1 MPa of hydrogen. After completion of the preformation of the hydrido complexes, the hydroformylation reaction was started with an olefin injection.

FTIR spectra were recorded between $\tilde{\nu} = 3950$ and 700 cm^{-1}, and the spectral resolution was set at 2 cm^{-1}. For one FTIR spectrum, ten scans were collected (double-sided, forward–backward) with the mirror speed set at 40 kHz. Time intervals between two measurements were 37 s for the first 120 min and 67 s after that period. For the GC analyses, a 7890A GC System from Agilent Technologies with a Petrocol DH 150 column (Supelco, Inc.) was used.

Acknowledgements

We thank the state of Mecklenburg–Western Pomerania and the German Federal Ministry for Education and Research for funding this work.

Keywords: hydroformylation · IR spectroscopy · kinetics · operando · rhodium

[1] a) O. Roelen, DE 849548, (1938/1952); b) J. F. Young, J. A. Osborn, F. A. Jardine, G. Wilkinson, *J. Chem. Soc., Chem. Commun.* **1965**, 131–132; c) B. Cornils, in *New Syntheses with Carbon Monoxide* (Ed.: J. Falbe), Springer, Berlin, **1980**; d) B. Cornils, W. A. Herrmann, M. Rasch, *Angew. Chem.* **1994**, *106*, 2219–2238; *Angew. Chem. Int. Ed. Engl.* **1994**, *33*, 2144–2163; e) *Rhodium Catalyzed Hydroformylation* (Eds.: P. W. N. M. Van Leeuwen, C. Claver), Kluwer, Dordrecht, **2000**; f) C. D. Frohning, C. W. Kohlpaintner, H.-W. Bohnen, in *Applied Homogeneous Catalysis with Organometallic Compounds* (Eds.: B. Cornils, W. A. Herrmann), 2ednd edWiley-VCH, Weinheim, **2002**.

[2] a) R. F. Heck, D. S. Breslow, *J. Am. Chem. Soc.* **1961**, *83*, 4023–4027; b) R. F. Heck, D. S. Breslow, *J. Am. Chem. Soc.* **1962**, *84*, 2499–2502; c) R. F. Heck, *Acc. Chem. Res.* **1969**, *2*, 10–16; d) D. Evans, J. A. Osborn, G. Wilkinson, *J. Chem. Soc. A* **1968**, 3133–3142; e) C. K. Brown, G. Wilkinson, *J. Chem. Soc. A* **1970**, 2753–2764.

[3] a) V. Agabekov, W. Seiche, B. Breit, *Chem. Sci.* **2013**, *4*, 2418–2422; b) A. R. Almeida, A. F. Peixoto, M. J. F. Calvete, P. M. P. Góis, M. M. Pereira, *Curr. Org. Synth.* **2011**, *8*, 764–775; c) I. Piras, R. Jennerjahn, R. Jackstell, A. Spannenberg, R. Franke, M. Beller, *Angew. Chem.* **2011**, *123*, 294–298; *Angew. Chem. Int. Ed.* **2011**, *50*, 280–284; d) I. Fleischer, L. Wu, I. Profir, R. Jackstell, R. Franke, M. Beller, *Chem. Eur. J.* **2013**, *19*, 10589–10594; e) L. C. Matsinha, P. Malatji, A. T. Hutton, G. A. Venter, S. F. Mapolie, G. S. Smith, *Eur. J. Inorg. Chem.* **2013**, 4318–4328; f) J. Pospech, I. Fleischer, R. Franke, S. Buchholz, M. Beller, *Angew. Chem.* **2013**, *125*, 2922–2944; *Angew. Chem. Int. Ed.* **2013**, *52*, 2852–2872; g) K. J. L. Chang, P. D. Nichols, S. Blackburn, *Lipid Technol.* **2013**, *25*, 199–203; h) O. Diebolt, C. Mueller, D. Vogt, *Catal. Sci. Technol.* **2012**, *2*, 773–777; i) S. Li, K. Huang, J. Zhang, W. Wu, X. Zhang, *Org. Lett.* **2013**, *15*, 3078–3081.

[4] a) O. Diebolt, H. Tricas, Z. Freixa, P. W. N. M. van Leeuwen, *ACS Catal.* **2013**, *3*, 128–137; b) H. Tricas, O. Diebolt, P. W. N. M. van Leeuwen, *J. Catal.* **2013**, *298*, 198–205; c) S. Güven, B. Hamers, R. Franke, M. Priske, M. Becker, D. Vogt, *Catal. Sci. Technol.* **2014**, *4*, 524–530; d) S. Güven, M. M. L. Nieuwenhuizen, B. Hamers, R. Franke, M. Priske, M. Becker, D. Vogt, *ChemCatChem* **2014**, *6*, 603–610.

[5] R. Franke, D. Selent, A. Börner, *Chem. Rev.* **2012**, *112*, 5675–5732.

[6] a) *Mechanisms in Homogeneous Catalysis* (Ed.: B. Heaton), Wiley-VCH, Weinheim, **2005**; selected recent publications: b) M. Garland, G. Li, L. Guo, *ACS Catal.* **2012**, *2*, 2327–2334; c) O. Diebolt, P. W. N. M. van Leeuwen, P. C. J. Kamer, *ACS Catal.* **2012**, *2*, 2357–2370; d) E. R. Nelsen, C. R. Landis, *J. Am. Chem. Soc.* **2013**, *135*, 9636–9639; e) C. J. Koeken, L. J. P. van den Broeke, B.-J. Deelman, J. T. F. Keurentjes, *J. Mol. Catal. A* **2011**, *346*, 1–11.

[7] C. Kubis, R. Ludwig, M. Sawall, K. Neymeyr, A. Börner, K.-D. Wiese, D. Hess, R. Franke, D. Selent, *ChemCatChem* **2010**, *2*, 287–295.

[8] C. Kubis, D. Selent, M. Sawall, R. Ludwig, K. Neymeyr, W. Baumann, R. Franke, A. Börner, *Chem. Eur. J.* **2012**, *18*, 8780–8794.

[9] M. Sparta, K. J. Børve, V. R. Jensen, *J. Am. Chem. Soc.* **2007**, *129*, 8487–8499.

[10] a) A. Van Rooy, E. N. Orij, P. C. J. Kamer, P. W. N. M. Van Leuuwen, *Organometallics* **1995**, *14*, 34–43; b) A. A. Dabbawala, H. C. Bajaj, R. V. Jasra, *J. Mol. Catal. A* **2009**, *302*, 97–106; c) A. Van Rooy, E. N. Orij, P. C. J. Kamer, F. Van den Aardweg, P. W. N. M. Van Leuuwen, *J. Chem. Soc. Chem. Commun.* **1991**, 1096–1097; d) M. Garland, P. Pino, *Organometallics* **1991**, *10*, 1693–1704; e) C. Fyhr, M. Garland, *Organometallics* **1993**, *12*, 1753–1764; f) J. Feng, M. Garland, *Organometallics* **1999**, *18*, 417–427.

[11] a) S. S. Divekar, R. M. Deshpande, R. V. Chaudhari, *Catal. Lett.* **1993**, *21*, 191–200; b) B. M. Bhanage, S. S. Divekar, R. M. Deshpande, R. V. Chaudhari, *J. Mol. Catal. A* **1997**, *115*, 247–257; c) B. Heil, L. Markó, *Chem. Ber.* **1968**, *101*, 2209–2214; d) M. Rosales, A. González, Y. Guerrero, I. Pacheco, R. A. Sánchez-Delgado, *J. Mol. Catal. A* **2007**, *270*, 241–249.

[12] For other studies that have used 3,3-dimethyl-1-butene as a substrate, see, for example: a) M. Garland, G. Bor, *Inorg. Chem.* **1989**, *28*, 410–413; b) M. Garland, *Organometallics* **1993**, *12*, 535–543; c) C. Li, E. Widjaja, M. Garland, *J. Catal.* **2003**, *213*, 126–134; d) B. Moasser, W. L. Gladfelter, D. C. Roe, *Organometallics* **1995**, *14*, 3832–3838 and ref. [10d].

[13] M. F. Faggin, M. A. Hines, *Rev. Sci. Instrum.* **2004**, *75*, 4547–4553.

[14] A. Van Rooy, P. C. J. Kamer, P. W. N. M. Van Leeuwen, K. Goubitz, J. Franje, N. Veldman, A. L. Spek, *Organometallics* **1996**, *15*, 835–847.

[15] The hydrogenolysis of normal and iso acyl–rhodium intermediates can proceed at different rates, even if the individual reaction orders with respect to [CO] are equal; see ref. [10 f].

[16] R. Crous, M. Datt, D. Foster, L. Bennie, C. Steenkamp, J. Huyser, L. Kirsten, G. Steyl, A. Roodt, *J. Chem. Soc. Dalton Trans.* **2005**, 1108–1116.

[17] a) K. Neymeyr, M. Sawall, D. Hess, *J. Chemometrics* **2010**, *24*, 67–74; b) M. Sawall, A. Börner, C. Kubis, D. Selent, R. Ludwig, K. Neymeyr, *J. Chemometrics* **2012**, *26*, 538–548.

[18] An axial coordination of the phosphorus ligand has been documented for corresponding triphenylphosphane complexes of rhodium and cobalt; see, for example: a) J. Zhang, M. Poliakoff, M. W. George, *Organometallics* **2003**, *22*, 1612–1618; b) P. C. Ford, S. M. Massik, *Coord. Chem. Rev.* **2002**, *226*, 39–49; c) S. M. Massick, J. G. Rabor, S. Elbers, J. Marhenke, S. Bernhard, J. J. Schoonover, P. C. Ford, *Inorg. Chem.* **2000**, *39*, 3098–3106; d) J. Somlyai-Haáz, F. Haáz, V. Galamb, A. Benedetti, C. Zucci, G. Pályi, T. Krümmling, B. Happ, T. Bartik, *J. Organomet. Chem.* **1991**, *419*, 205–217; e) I. Kovács, F. Ungváry, *Coord. Chem. Rev.* **1997**, *161*, 1–32.

[19] Such relationship is also known from unmodified hydroformylation of structurally different alkenes; see: G. Liu, R. Volken, M. Garland, *Organometallics* **1999**, *18*, 3429–3426 and refs. [10d,f].

[20] See the Supporting Information for the full set of the concentration profiles, which were determined for all the different carbon monoxide pressures applied.

[21] See the Supporting Information for the derivation of the kinetic model and F. G. Helfferich in *Comprehensive Chemical Kinetics, Vol. 38* (Ed.: N. J. B. Green), Elsevier Science Amsterdam, **2004**.

[22] See the Supporting Information for a comparison of the entire set of the concentration profiles of the rhodium complexes obtained at the different carbon monoxide pressures applied.

[23] A. Cornish-Bowden, *Fundamentals of Enzyme Kinetics*, Portland Press, London, 3edrd ed**2004**.

[24] a) S. Kozuch, J. M. Martin, *ChemPhysChem* **2011**, *12*, 1413–1418; the traditional concept of individual, early, and late rate-determining elemen-

tary steps, which is still used in transition-metal catalysis, needs to be modified; see, for example: b) E. Zuidema, L. Escorihuela, T. Eichelsheim, J. J. Carbó, C. Bo, P. C. J. Kamer, P. W. N. M. van Leeuwen, *Chem. Eur. J.* **2008**, *14*, 1843 – 1853.

[25] a) C. Bergounhou, D. Neibecker, R. Mathieu, *J. Mol. Catal. A* **2004**, *220*, 167 – 182; b) D. G. Blackmond, *Angew. Chem.* **2005**, *117*, 4374 – 4393; *Angew. Chem. Int. Ed.* **2005**, *44*, 4302 – 4320; c) H.-J. Drexler, A. Preetz, T. Schmidt, D. Heller in *The Handbook of Homogeneous Hydrogenation* (Eds.: J. G. de Vries, C. J. Elsevier), Wiley-VCH, Weinheim, **2007**, pp. 257 – 293.

[26] The detailed spectroscopic identification of metal carbonyl complexes related to nonmodified rhodium-catalyzed homogeneous hydroformylation and the respective kinetic evaluation, has been exemplified repeatedly by Garland and co-workers; see, for example, the references cited in [15] and [19]; furthermore, by the same authors, the semibatch experimental design was shown to be of strong benefit to gain reliable kinetic information and identify the transition-metal carbonyl complexes present in very low concentrations: a) E. Widjaja, C. Li, M. Garland, *Organometallics* **2002**, *21*, 1991 – 1997; b) C. Li, E. Widjaja, W. Chew, M. Garland, *Angew. Chem.* **2002**, *114*, 3939 – 3943; *Angew. Chem. Int. Ed.* **2002**, *41*, 3785 – 3789.

Received: March 7, 2014
Published online on July 31, 2014